A Method for Obtaining a Low Resolution 3D Reconstruction from Very Noisy Projections

Luis Gerardo de la Fraga § José María Carazo §

Gabor T. Herman ‡

§ BioComputing Unit, Centro Nacional de Biotecnología-CSIC,
Campus Universidad Autónoma, 28049 Madrid, Spain.

‡ Medical Image Processing Group, Department of Radiology,
University of Pennsylvania, Philadelphia, PA 19104, USA.

E-mail: `fraga@tango.cnb.uam.es`

Abstract

In the course of our research towards high resolution 3-D reconstruction of biological macromolecules in electron microscopy, we have developed a methodology for reconstructing a preliminary low resolution volume from 2-D projection images with signal-to-noise ratio less than one. We have concentrated on solving the translational alignment of the tilted projections. This first reconstructed volume can be used to perform a refinement of the geometry for the entire set of projections. We demonstrate the method on three synthetic models of proteins.

1 Introduction

By a *projection* of a *volume* (a three-dimensional object) we understand a collection of estimates of line integrals through the volume along a set of lines which are all perpendicular to a particular plane. Three-dimensional (3D) reconstruction is the process of estimating the volume from a number of projections. In order to be able to do 3D reconstruction, we need information regarding the location of the lines relative to a coordinate system fixed to the volume. Given an image representing a projection, the location of lines perpendicular to the projection plane at the individual pixels can be calculated, provided that we know the two Euler angles of the normal to the projection plane (we refer to these as the *tilt* and the *rotation*) and the two coordinates of the location in the plane onto which the origin of the volume coordinate system is projected. This problem is automatically solved in medical 3D reconstruction [Herman, 1980], since in that application all the projections are taken of a single volume (the patient) and so the coordinate system of the volume can be assumed to be that of the instrument which collects the data.

In 3D reconstruction of biological macromolecules from electron microscope projections the data collection method is quite destructive, severely limiting our ability of producing multiple projections of the same particle. On the other hand, we may assume that all particles are identical, and so we can consider a single projection of a particular particle to be one of the projections of the volume to be reconstructed. The problem is that we have very limited control of the orientation of the particles in the instrument and so we have to make use of the projection images themselves to estimate the Euler angles and coordinates mentioned above.

The random-conical reconstruction scheme is much used for this purpose [Radermacher, 1988, Lambert et al., 1995]. This technique uses a pair of micrographs (the first tilted and the second untilted) of a specimen containing many particles, prepared in such a way that all the particles assume a preferred orientation with respect to the specimen support. If this is performed successfully, each particle image seen in the tilted micrograph is a projection with a fixed tilt, but unknown rotation. The untilted view (in which the rotation of the volume around the common axis of the particles is reflected by rotation by the same angle in the projection) can be used to estimate the rotation. Also, by averaging the unrotated versions of the particles in the untilted view, we can get a high quality estimate of the untilted projection and consequently a good estimate of the projection of the origin of the volume coordinate system. (Here we may assume that this origin is at the centroid of the volume and make use of the fact that, if noise is negligible, then the centroid of the projection is a good estimate of the centroid of the volume.) Finally, one may estimate the coordinates of the projection of the origin in the tilted projection images by the the so-called *cosine stretching* [Radermacher, 1988, Carazo and Frank, 1988] procedure: the tilted projection is stretched by the factor $1/\cos(\varphi)$ in the direction perpendicular to the tilt axis, where φ is the tilt angle, and cross-correlated with the averaged untilted projection. This procedure appears to work well for flat volumes, that is for those whose thickness perpendicular to the projection plane is much less than the dimensions in the plane. The random-conical reconstruction scheme has found wide popularity because, in principle, it solves the problem of finding the relative orientations of the different projections.

However, the methodology described in the previous paragraph produces a less than perfect estimation of the geometrical parameters of the projections with respect to the assumed fixed coordinate system attached to the volume for three reasons. (i) The tilt angle in reality is not identical for all particles, but encompasses a range, of possibly as much as 20°, due to the support not being completely flat. (ii) The rotation angles are determined from the untilted image, in which the particles have been previously exposed (while taking the tilted image) to the electron beam and may have been damaged. (iii) The location of the projection of the origin of the assumed coordinate system (attached to the particles) may be incorrectly determined by the cosine stretching procedure for volumes which are not very flat.

All these limitations can be taken care of by the use of a *refinement* method [Penczek et al., 1994, Radermacher, 1994]. The essence of such a method is the following: get an estimated volume, calculate the needed geometrical parameters by the consistency of the tilted projections with the estimate, reconstruct with the new parameters and repeat until convergence. The problem is how to start this iterative process; i.e., how to obtain the first estimated volume. To our knowledge this problem has not been carefully discussed in the literature to date. Our paper proposes a methodology for solving it.

In this methodology we do not try to correct for (i) and (ii) above; for the first reconstruction we assume that the tilt and rotation angles obtained by the standard method are correct. Our contribution is that we solve the third problem (as well as we can), by identifying in the projection image the location onto which the volume centroid projects purely from the projection image. We use classical procedures of image processing, that may nevertheless be applied to typical images obtained in a transmission electron microscope, with a signal-to-noise ratio less than one. Table 1 shows that (at least in the case of accurate tilt and rotation angles) our estimates of the locations in noisy projections of the projections of centroids of volumes are clearly superior to those provided by the cosine stretching procedure.

2 Method description

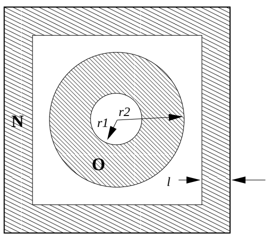

Figure 1: Image regions

We are given a set of images which represent the projections of the volume (e.g., Fig. 2(a)). All steps below are applied to each projection image. The objective is to identify in the projection image those pixels which contain signal (i.e., for which the corresponding line integral of the volume would not be zero even in the noiseless case). We use only these pixels to estimate the location of the projection of the centroid of the volume (which, in the noiseless case, is the centroid of the projection). In a final step we check for the consistency of the particular projection with the rest, so as to discard those projections (prior to reconstruction) which have contained too much noise for our procedure to work.

1. We start by applying to the original image $f(x,y)$ the smoothing:

$$g_1(x,y) = \frac{1}{9}\sum_{i=-1}^{1}\sum_{j=-1}^{1} f(x+i,y+j) \qquad \text{for} \quad 0 < x < N-1, \quad 0 < y < N-1 \tag{1}$$

   where N is the size of our square-shaped images; see Fig. 2(b)

2. We find the mean and standard deviation of both the background region, considered to contain only noise, m_b, σ_b, and the object region m_o, σ_o on the original $f(x,y)$ image. As we can see in Fig. 1, the object zone is between r_1 and r_2 radius, and the background zone is at the border as specified by the parameter l. Then we find a value m such that

$$\frac{m_o - m}{\sigma_o} = \frac{m - m_b}{\sigma_b} \tag{2}$$

We make a new image $g_2(x,y)$ as follows:

$$g_2(x,y) = \begin{cases} 0 & \text{if} \quad g_1(x,y) \geq m_o, \\ 1 & \text{if} \quad \frac{m_o+m}{2} \leq g_1(x,y) < m_o, \\ 2 & \text{if} \quad m \leq g_1(x,y) < \frac{m_o+m}{2}, \\ 3 & \text{if} \quad \frac{m_b+m}{2} \leq g_1(x,y) < m, \\ 4 & \text{if} \quad m_b \leq g_1(x,y) < \frac{m_b+m}{2}, \\ 5 & \text{if} \quad g_1(x,y) < m_b. \end{cases} \tag{3}$$

As an example of this six-tone image see Fig. 2(c).

3. Now we binarize the image $g_2(x,y)$ of eq. (3) by applying the following subroutine. As input to the subroutine we have the $g_2(x,y)$ image. As output we get a new image $g_3(x,y)$.

   for $1 \leq s \leq 5$ **do**

   (a) **if** $g_2(x,y) = 0$ or 5 **then** **set** $g_3(x,y) = g_2(x,y)$;

   (b) **else**
   Calculate the average, $\text{ave}(x,y)$, in the four-connected neighborhood at x, y

   $$\text{ave}(x,y) = \frac{1}{5}\left[\sum_{i=-1}^{1} g_2(x+i,y) + g_2(x,y-1) + g_2(x,y+1)\right] \tag{4}$$

      i. **if** $\text{ave}(x,y) \leq 0.5s$ **then** **set** $g_3(x,y) = 0$;

      ii. **else if** $\text{ave}(x,y) \geq 5 - 0.5s$ **then** **set** $g_3(x,y) = 5$;

      iii. **else** **set** $g_3(x,y) = g_2(x,y)$;

      iv. **endif**

   (c) **endif**

   (d) **if** $s \neq 5$ **then** **Copy** image $g_3(x,y)$ to image $g_2(x,y)$

   (e) **endif**

   endfor

   Upon the completion of this subroutine we obtain a two-valued image $g_3(x,y)$ that, as an example, can be see in Fig. 2(d).

4. A mask is extracted as follows. Search for a pixel in the annulus between r_1 and r_2 (see Fig. 1) for which g_3 has value 0. If this search is not successful, then a mask can not be extracted. If the search is successful, then we use a modification of the algorithm *"Filling by connectivity"* [Pavlidis, 1982] to find the component of the 0-valued pixels in g_3 containing the found pixel. If this component is over the image border, then we consider that there is no mask. Otherwise, we assign to the pixels inside the mask the value 1 and all the rest pixels are set to 0. The resulting image can be seen in Fig. 2(e).

5. We dilate the mask by attaching to it all the points which are originally outside it, but are 4-adjacent to it. The result of the dilation is illustrated in Fig. 2(f).

6. Finaly, we calculate the centroid of the final mask [Russ, 1994]

   $$\text{C.G.}_{\cdot x} = \frac{\sum_i g_1(x_i,y_i) \cdot x_i}{\sum_i g_1(x_i,y_i)} \qquad \text{C.G.}_{\cdot y} = \frac{\sum_i g_1(x_i,y_i) \cdot y_i}{\sum_i g_1(x_i,y_i)} \tag{5}$$

   where g_1 is the smoothed image and x_i, y_i are related to the positions where pixel values of the final image, g_f, are equal to 1.

7. Classification of all the masks. We use two measures to perform it: The *Form Factor* (F.F.) and the *Equivalent Diameter* (E.D.), defined as:

   $$\text{F.F.} = \sqrt{\frac{1}{Area}\left[\sum_i (x_i - \text{C.G.}_{\cdot x})^2 + \sum_i (y_i - \text{C.G.}_{\cdot y})^2\right]} \qquad \text{E.D.} = \sqrt{\frac{4}{\pi} Area} \tag{6}$$

   And we choose the *bigger cluster* that appear on a map representing F.F. versus E.D. for each of the images.

(a) Original image | (b) Smoothed | (c) Six tones | (d) Refined | (e) Extracted | (f) Dilated

Figure 2: A application example for all the process. Details in the text.

3 Experiment

We start with three volume phantoms:

1. CCT, showed in Fig. 3(a), is a synthetic model that was constructed from 2D views of the real CCT [Marco et al., 1994] protein.

2. BCI, in Fig. 3(b), is a synthetic model of a thick protein and

3. fBCI, in Fig. 3(c), is a flat version of the BCI phantom.

The CCT phantom presents a cylindrical eight-fold symmetry. BCI and fBCI present a cylindrical four-fold symmetry. This characteristic shall be useful to obtain a better reconstruction.

For each phantom we take 65 reprojections at $55°$ in tilt angle and $n \cdot 2\pi/65$, $0 \leq n < 65$, in the azimuthal angle (according to a conical-tilt geometry). We added to each reprojected image a zero-mean Gaussian noise to get a fractional noise level of 0.8 [Farrow and Ottensmeyer, 1992]: The level of noise added to each projection is expressed as the ratio between the standard deviation of the noise added and the average intensity range for all simulated images. The fnl=0.8 correspond approximately to a signal-to-noise ratio of 0.3. Examples of untilt reprojections, without noise, for each phantom can be seen in the first row in Fig. 4; tilt reprojections are in the second row in the same Fig. 4. These images plus noise added are in the third row. The Fig. 2(a) is the same that the second image in the third row.
We then apply the method described in Section 2.
Finally, and as a final check of the whole procedure, with the set of images in which we were able to find the centroid, we perform a 3D reconstruction using the "weighted back-projection" algorithm [Radermacher, 1988].

The proposed method was programmed in ANSI-C programming language. The software package XMIPP [Marabini et al., 1996] was used to perform the phantoms, reprojections and reconstructions. The WEB [Frank et al., 1996] package was used to make the surface visualization used in Figs. 3 and 5.

4 Results

To test our method, we compare it with the usual *cosine stretching* for alignment the tilted images with the untilted pairs (see second column on Table 1). The errors was calculated using eq. (7), this is, the mean squared error between the correct location of the centroid and those other coordinates calculated by our method.

$$\text{error} = \frac{(val_{ok} - val_{new})^2}{N} \tag{7}$$

N in Table 1 is the final number of images in the process. The mask's classification only rejected images in fBCI case. In Fig. 6(a) we see that all the masks form a single cluster. This was also true for the BCI phantom. For the fBCI (Fig. 6(b)) however we see clearly two clusters. In this case, the choice of the "correct" cluster was just to take the bigger one (top-right).

5 Conclusion

We have designed a new methodology for translational alignment of a set of very noisy projections of a volume. The methodology allow to generate a low-resolution volume suitable to be used to a refinement

(a) CCT

(b) BCI

(c) fBCI

Figure 3: Volume phantoms

Figure 4: Image examples

(a) CCT

(b) BCI

(c) fBCI

Figure 5: 3D reconstructed phantoms

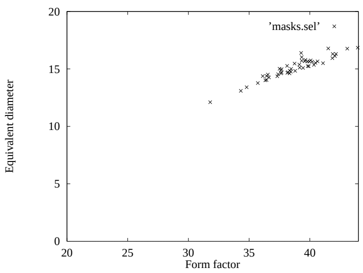

(a) CCT case

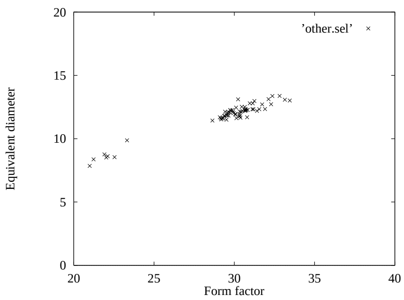

(b) fBCI case

Figure 6: Classification results

Specimen	Error with correlation masks		Error with our method		N
CCT	$dx = 42.215$	$dy = 2.809$	$dx = 1.687$	$dy = 0.594$	51
BCI	$dx = 236.735$	$dy = 5.173$	$dx = 1.197$	$dy = 0.875$	57
fBCI	$dx = 1.825$	$dy = 0.881$	$dx = 0.240$	$dy = 0.478$	57

Table 1: Simulation results

procedure of its geometry. We have demonstrated that the method works for images with very low signal-to-noise ratios.

Acknowledgments

This work has been partly supported by grant BIO95-0768 from de Comisión Interministerial de Ciencia y Tecnología, Spain, to Dr. J.M. Carazo, and by NIH grant HL28438 to Dr. Herman. Mr. L.G. de la Fraga holds a partial predoctoral studenship granted by CONACYT, México; and by Universidad Autónoma del Estado de Morelos, México. Our cooperation has been supported by NATO grant CRG 960070.

References

[Carazo and Frank, 1988] Carazo, J. M. and Frank, J. (1988). Three-dimensional matching of macromolecular structures obtained from electron microscopy. *Ultramicroscopy*, 25:13–22.

[Farrow and Ottensmeyer, 1992] Farrow, N. A. and Ottensmeyer, F. P. (1992). A posteriori determination of relative projection directions of arbitrarily oriented macromolecules. *J. Opt. Soc. Am. A*, 9(10):1749–1760.

[Frank et al., 1996] Frank, J., Radermacher, M., Penczek, P., Zhu, J., Li, Y., Ladjadj, M., and Leith, A. (1996). SPIDER and WEB: Processing and visualization of images in 3D electron microscopy and related fields. *J. of Struct. Biol.*, 116:190–199.

[Herman, 1980] Herman, G. T. (1980). *Image Reconstruction from Projections: The Fundamentals of Computerized Tomography.* Academic Press.

[Lambert et al., 1995] Lambert, O., Boisset, N., Taveau, J.-C., Préaux, G., and Lamy, J. N. (1995). Three-dimensional recontruction of the α_D and β_C-hemocyanins of *helix pomatia* from frozed-hidrated specimens. *J. Mol. Biol.*, 248:431–448.

[Marabini et al., 1996] Marabini, R., Masegosa, I. M., San Martin, M. C., Marco, S., de la Fraga, L. G., Vaquerizo, C., and Carazo, J. M. (1996). Xmipp: An image processing package for electron microscopy. *J. of Struct. Biol.*, 116:237–240.

[Marco et al., 1994] Marco, S., Carrascosa, J. L., and Valpuesta, J. M. (1994). Reversible interaction of β-actin along the channel of the TCP-1 cytoplasmic chaperonin. *Biophysical Journal*, 67:364–368.

[Pavlidis, 1982] Pavlidis, T. (1982). *Algorithms for Graphics and Image Processing.* Computer Science Press.

[Penczek et al., 1994] Penczek, P. A., Grassuni, R. A., and Frank, J. (1994). The ribosome at improved resolution: new techniques for for merging and orientation refinement in 3D cryo-electron microscopy of biological particles. *Ultramicroscopy*, 53:251–270.

[Radermacher, 1988] Radermacher, M. (1988). The three-dimensional reconstruction of single particles from random and non-random tilt series. *J. Electron Microsc. Tech.*, 9:359–394.

[Radermacher, 1994] Radermacher, M. (1994). Three-dimensional reconstruction from random projections: Orientational alignment via Radon transforms. *Ultramicroscopy*, 53:121–136.

[Russ, 1994] Russ, J. C. (1994). *The Image Processing Handbook. 2nd. ed.* CRC Press.